AUT Journal of Electrical Engineering

AUT J. Elec. Eng., 52(2) (2020) 147-158
DOI: 10.22060/eej.2020.18115.5343

Backhaul-aware Decoupled Uplink and Downlink User Association, and Power Control in Fi-Wi HetNets

R. Hashemi[1], H. Beyranvand[2,*]

[1]MSc, Electrical Engineering Department, Amirkabir University of Technology (Tehran Polytechnic), Tehran, Iran
[2]PhD, Electrical Engineering Department, Amirkabir University of Technology (Tehran Polytechnic), Tehran, Iran

ABSTRACT: Decoupling the uplink and downlink user association improves the throughput of heterogeneous networks (HetNets) and balances the traffic load of macro- and small- base stations. Recently, fiber-wireless HetNets (FiWi-HetNets) have been considered as viable solutions for access networks. To improve the accuracy of user association and resource allocation algorithms in FiWi-HetNets, the capacity limitation of various backhaul technologies must be considered. In this paper, we investigate the backhaul-aware decoupled uplink/downlink (UL/DL) user association, subcarrier allocation, and power control optimization problem in FiWi-HetNets. In our system model, fiber and millimeter wave (mmWave) links are used as backhaul of base stations, and the backhaul capacity limitation and minimum required transmission rate (R_min) are modeled in the optimization problem. As the formulated optimization problem is non-convex, we present a heuristic algorithm to divide the main problem into two sub-problems that are solved iteratively. The proposed algorithms are evaluated through exhaustive simulations. The results indicate that decoupling UL/DL user association improves the sum rate of FiWi-HetNets. Besides, we evaluate the effect of backhaul capacity limitation and R_min on the sum rate of FiWi-HetNets. The effect of upgrading fiber backhaul technology is also investigated to evaluate the role of fiber backhaul on the sum rate of the radio access network.

Review History:

Received: 2020-03-15
Revised: 2020-08-10
Accepted: 2020-08-11
Available Online: 2020-12-01

Keywords:

Fiber-Wireless (Fi-Wi) Heterogeneous Networks
Decoupled Uplink and Downlink
Power control and Subcarrier Allocation
Passive Optical Networks

1- Introduction

The emergence of new technologies such as tactile Internet and virtual reality [1] have exacerbated the ever-increasing demand for higher Quality of Service (QoS) transmission in access and core networks. International Telecommunication Union (ITU) has defined the IMT-2020 to specify the main requirements of fifth-generation (5G) radio access networks (RANs) [2, 3]. In November 2016, Full Service Access Network (FSAN) organization[1] has released the standardization roadmap of optical fiber access networks specifying the time-line and main features of the so-called passive optical network (PON) architecture [4, 5]. In the FSAN roadmap, industry trends such as Software Defined Networking (SDN), Network Function Visualization (NFV), 5G, and Internet of Things (IoT) have been taken into account, which highlights the convergence of radio and fiber technologies in the next generation Broadband Access Networks (BANs). Recently, Fiber-Wireless (FiWi) heterogeneous networks (FiWi-HetNets) have been introduced to integrate RAN and PON technologies and realize efficient and ultra-fast BANs [6-9]. For instance, [10] proposed a mobile cloud computing model empowered FiWi enhanced LTE-A HetNets architecture. The authors in [11] designed an energy-efficient FiWi network based on wireless sensor networks.

In 5G RAN, the densification technique, i.e., ultra-dense deployment of small base stations (SBSs) besides macro base stations (MBSs), has been proposed to improve the spectral efficiency of BANs [12]. Although densification improves aerial transmission capacity, however, it raises the so-called backhauling bottleneck [13, 14]. In heterogeneous RANs, referred to as HetNets, SBSs are connected to the core network through MBSs or gateway. The link between SBSs and either MBS or gateway is referred to as *backhaul* or *fronthaul* link[2]. Optical fiber, free-space optic link, radio frequency wireless link, twisted-pair wire, or coaxial cable can be used as backhaul (BH) link in HetNets [15, 16]. It has been shown that the capacity limitation of backhaul affects the QoS features of mobile users [7], thus, backhaul-aware resource allocation in FiWi-HetNets is of paramount importance.

Recently the concept of decoupling uplink (UL) and

1 FSAN is a forum through which telecom operators, equipment manufacturers, and chip vendors can collaborate to promote the development of fiber-optic access networks standards recommended by ITU.

2 It should be noted that in the terminology of cloud-radio access network (C-RAN) the word fronthaul indicates the link between remote radio head (RRH) and baseband unit (BBU), while the term backhaul means the backbone infrastructure connecting BBUs to the core network. However, in this study, we use the term backhaul to indicate either fiber links between small base station and central office or wireless links between small base station and macro base station.

*Corresponding author's email: beyranvand@aut.ac.ir

Table 1. Comparing the most related studies (OP: Optimization Problem, SG: Stochastic Geometry).

Reference	[18, 20, 21]	[22]	[24]	[7]	Our work
Methodology	SG	OP	OP	OP	OP
Considering BH limitation	×	×	✓	✓	✓
Considering minimum required rate	×	×	✓	×	✓
Power control	×	×	✓	×	✓
Studying decoupling gain	✓	✓	×	×	✓
PON topology	×	×	×	✓	✓
Scenario	DL or UL	DL and UL	DL	DL	DL and UL

downlink (DL) user association has been introduced in HetNets to achieve higher throughput and load balancing [17]. The performance improvement obtained with UL/DL decoupling is due to the fact that HetNets are more disperse in transmit power of nodes. Therefore, analyzing the decoupling gain in resource allocation and user association problems in FiWi-HetNets, while taking into account the QoS requirements of each user as well as considering the limitation of backhaul capacity is of great importance, which has not been investigated in previous studies. Thus, in this paper, we are motivated to investigate this problem and propose new algorithms to solve it.

1-1- Related Work

The authors in [18] investigated the distribution of signal-to-interference-plus-noise ratio (SINR) and rate formula for the UL of a k-tier heterogeneous network using the stochastic geometry analysis. They showed that decoupling UL and DL associations result in increasing the rate coverage. In [19], the probability distribution functions of SINR and spectral efficiency in the DL of a HetNet were derived, and the concept of cell biasing was introduced to tackle the congestion of users in macrocells. By employing the stochastic geometry analysis, the authors in [20] solved user association problems with either maximum biased received signal power or maximum achievable rate criteria in the DL and UL association procedure of a 2-tier HetNet. In addition, the authors studied the UL/DL decoupling, but without considering the backhaul capacity constraint and QoS requirements. In [21], the UL performance of HetNets in terms of achievable rate and spectral efficiency has been analytically evaluated using stochastic geometry. None of the aforementioned prior studies take into account the backhaul capacity limitation and QoS requirements.

By leveraging the concept of convex optimization, the authors in [22] investigated the optimization problem of decoupled UL/DL association with the objective of sum-rate maximization. In [23], the user association and resource allocation problem in DL of a 3-tier HetNet has been studied by maximizing the network utility function. Nevertheless, the backhaul capacity limitation and users' QoS requirements have not been considered in [22, 23]. The problem of DL user association and power control with the aim of load balancing by considering both the backhaul capacity limitation and users' QoS requirements has been studied in [24]. However, the authors did not solve the problem for UL transmission, and the UL/DL decoupling gain has not been investigated. Moreover, in [7], a backhaul-aware user association scheme for FiWi-LTE networks has been introduced for DL transmission without considering the QoS rate constraint.

On the other side, a large number of papers investigate the problem of resource allocation and power control in HetNets. Here, we only introduce the most relevant papers. The authors in [25] solved the problem of joint sub-channel assignment and power control in the UL of a HetNet, and the difference of convex (concave) approach has been used to find the sub-optimal solutions. In [26] and [27], by using the arithmetic geometric mean approximation (AGMA) the non-convex power allocation problem has been transformed into geometric programming (GP), and [27] considered the QoS requirements of the macro cell users in the proposed optimization problem. Table 1 shows a comparison of the most relevant recent studies.

1-2- Contributions and Organization

The main contribution of this paper is summarized as follows:

• To the best of our knowledge the optimization problem of resource block (RB) assignment, power control, and decoupled UL/DL user association in FiWi-HetNets has not been addressed so far. In particular, we formulate the optimization problem of backhaul-aware decoupled UL/DL user association, and joint RB assignment and power control in both UL and DL of a FiWi-HetNet by satisfying the users' QoS requirements.

• An efficient algorithm is presented to solve the introduced problem. Since the formulated problem is non-convex and non-tractable, we relax the integer association variables and

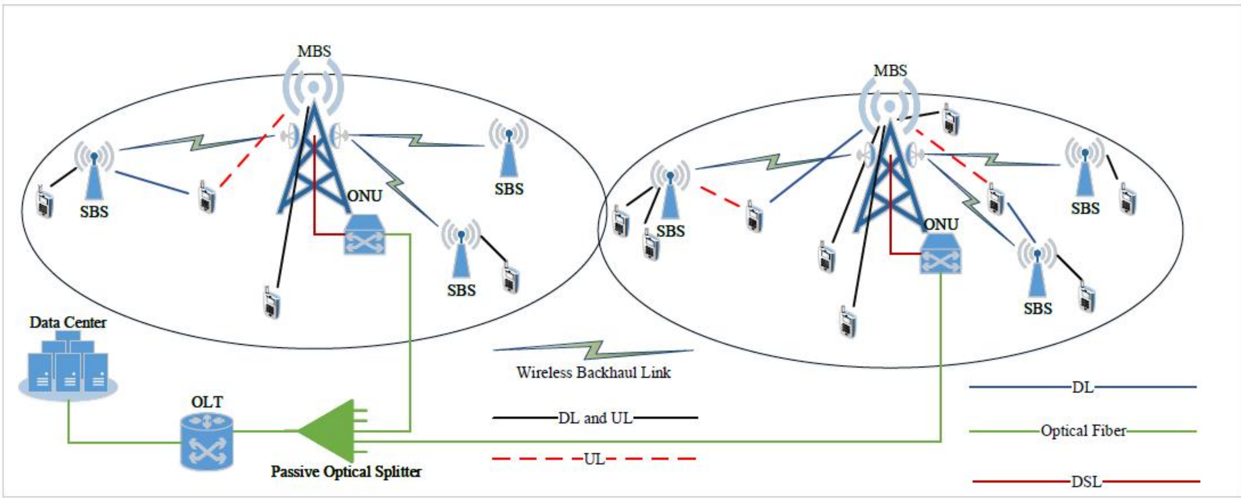

Fig. 1. Fi-Wi network architecture and system model.

separate the main problem into two sub-problems: **i)** decoupled UL/DL user association and RB assignment, and **ii)** UL and DL power control. The association problem is transformed into linear programming. To solve the second problem, we propose to use AGMA and geometric programming approach to find the sub-optimal solutions iteratively.

• Finally, we evaluate the proposed optimization problems and indicate that decoupling UL/DL association leads to higher throughput. We also show that by limiting the backhaul capacity of FiWi-HetNets, the QoS satisfaction of end-users is violated. In addition, we consider different variants of PON standards to evaluate the effect of the transmission rate of fiber backhaul in the aggregate throughput of FiWi-HetNets. We show that in low splitting ratios of PON technologies, the backhaul capacity of MBS is higher than its capacity at the air interface, and as a result upgrading PON technology does not impact its performance.

The rest of the paper is organized as follows. In Section 2, we present our system model. In Section 3, we formulate the optimization problem of user association, spectrum assignment, and power control in FiWi-HetNet. Then, in Section 4, we present the proposed algorithms to solve the non-convex problem formulated in the former section. In Section 5, numerical results are presented to evaluate the proposed algorithms and study the UL/DL decoupling gain in FiWi-HetNets. Finally, the paper is concluded in Section 6.

2- System Model

2-1- Network Architecture

In this paper, we consider FiWi-HetNet architecture that is the integration of radio access and fiber-optic access technologies, as depicted in Fig. 1.2. We employ PON architecture as a fiber access infrastructure to provide backhaul links for MBSs. This architecture has been standardized as a promising technology to realize fiber-to-the-x (FTTx) deployments, where the x stands for a home, building, neighborhood, or curb [6]. The main components of a PON are the optical line terminal (OLT), passive power splitter, and optical network units (ONUs). Generally, a PON has a tree-and-branch topology, in which the OLT and ONUs serve as the root and leave nodes, respectively. The OLT is located at the central office (CO) and performs resource allocation among ONUs, and ONUs reside at subscriber premises. In our model, the MBS is connected to an ONU serving a single PON subscriber.

In PON architecture, ONU is used in FTTB and FTTC deployments, whereas Optical Network Termination (ONT) is used for the case of FTTH. In general, ONU and ONT have the same networking functionality, however, ONU has more interfaces to support a number of subscribers, and ONT is a simple modem providing an Internet connection for only one subscriber.

Two families of standards have been recommended for PON by ITU and the Institute of Electrical and Electronics Engineers (IEEE) [5]. The Gigabit PON (GPON) and Ethernet PON (EPON) are the most popular PON technologies standardized by ITU and IEEE, respectively [28]. In this paper, we focus on the GPON and its newest variants. The GPON's requirements were defined by FSAN organization which was ratified by ITU and published as recommendation G.984 [29]. In the GPON standard, two separate wavelengths are allocated for UL and DL transmission, and in each wavelength time division multiple access (TDMA) technique is used to transmit data of multiple users, where the transmission rates in DL and UL are 2.5 Gbps and 1.25 Gbps, respectively. The 10 Gigabit-class variants of GPON, referred to as XG-PON and XGS-PON, have been defined by ITU in recommendations G.987.2 and G.9807.1, respectively [30]. The multiplexing technique of XG-PON and XGS-PON is the same as GPON, and the DL/UL transmission rates of XG-PON and XGS-PON are 10 Gbps/2.5 Gbps and 10 Gbps/10 Gbps, respectively.

Recently, ITU has published recommendation G.989 [31] to specify the second phase of the next-generation GPON, the so-called Next-Generation Passive Optical Network 2 (NG-PON2). In NG-PON2, multiple subscribers are served by utilizing hybrid time and wavelength division multiplexing

(WDM), where four wavelengths are utilized for DL, and in each wavelength 10 Gbps maximum peak rate is provided, thus, its total DL transmission rate is 40 Gbps [28]. In NG-PON2, two modes of 40 Gbps and 10 Gbps have been defined for UL transmission. In NG-PON2, in addition to the point-to-multi-point (P2MP) operation mode, the point-to-point (P2P) operation has been defined, which allocates the total bandwidth of a wavelength to a subscriber. The P2P mode is desirable for FiWi-HetNets to provide guaranteed bandwidth as a backhaul link of either MBSs or SBSs. In this study, we evaluate the effect of upgrading PON technology employed as the optical networking infrastructure of FiWi-HetNets by considering migration from GPON to NG-PON2.

In the RAN part of FiWi-HetNets, we consider a two-tier wireless network containing macro and small cells, in which the MBS has fiber backhaul interconnected to ONUs of PON, and SBSs are connected to MBS via mmWave backhaul. Although, SBSs can be connected to the core network via fiber backhaul, in this paper, without loss of generality of formulations and optimization framework, we consider only wireless backhauling for SBSs. Furthermore, we assume that MBSs and SBSs employ orthogonal frequency division multiple access (OFDMA) technique to share their bandwidth among served users, where frequency division duplexing (FDD) is used to transmit UL and DL signals. We denote the total UL and DL bandwidth of each base station (BS) by BW_UL and BW_DL, respectively.

The network architecture is indicated in Fig. 1. We assume two scenarios for users association: **1)** UL/DL decoupled in which the user equipment (UE) is associated with different BSs (MBS or SBS) in UL and DL, and **2)** UL/DL coupled association, which means that each UE is connected to the same BS in UL and DL. In the next section, the association problem is formulated in an optimization problem, and UEs are allowed to be associated either coupled or decoupled with the objective of rate maximization.

2-2- Backhaul Capacity Limitation

In what follows, we formulate the capacity of fiber and mmWave backhauls to model the backhaul capacity constraint in our optimization problem presented in the next section.

Fiber Backhaul Capacity: We inspire the capacity analysis presented in [32] to obtain the fiber backhaul capacity in different PON technologies. In TDMA based PON ($\ddot{E}=1$) and WDM based PON ($\ddot{E}>1$) technologies, the transmission rates allocated to i'th ONU in DL and UL transmission, $C_{ONU_i}^{DL}$ and $C_{ONU_i}^{UL}$, for fixed bandwidth allocation method are obtained as follows

$$C_{ONU_i}^{DL} = \frac{c_{PON}^{DL}}{\ddot{E}\, O_k}, \tag{1}$$

$$C_{ONU_i}^{UL} = \frac{c_{PON}^{UL}}{\ddot{E}\, O_k}, \tag{2}$$

where $\ddot{E}$ is the number of wavelengths used in PON, c_{PON}^{DL} and c_{PON}^{UL} denote the PON data rate (in bits/s) in DL and UL transmission, respectively, O_k indicates the number of ONUs served by OLT in k th wavelength. By calculating $C_{ONU_i}^{DL}$ and $C_{ONU_i}^{UL}$, the backhaul capacity of the MBS connected to i'th ONU is obtained.

mmWave Backhaul Capacity: We consider the achievable rate of mmWave wireless link between SBS and MBS to compute the capacity of mmWave backhaul, thus we have [33]

$$C_{\mathrm{mmWave}_s}^{UL} = \mathrm{BW}_{\mathrm{mmWave}}^{UL} \log\left(1+\mathrm{SINR}_{s,b}^{UL}\right), \tag{3}$$

$$C_{\mathrm{mmWave}_s}^{DL} = \mathrm{BW}_{\mathrm{mmWave}}^{DL} \log\left(1+\mathrm{SINR}_{s,b}^{DL}\right), \tag{4}$$

where $C_{\mathrm{mmWave}_s}^{UL}$ ($C_{\mathrm{mmWave}_s}^{DL}$), $\mathrm{BW}_{\mathrm{mmWave}}^{UL}$ ($\mathrm{BW}_{\mathrm{mmWave}}^{DL}$), and $\mathrm{SINR}_{s,b}^{UL}$ ($\mathrm{SINR}_{s,b}^{DL}$) are respectively the mmWave backhaul capacity of s'th SBS, the bandwidth of mmWave backhaul link, and the SINR of wireless link between s'th SBS and MBS b in UL (DL) transmission.

2-3-Notations

In this paper, we assume that each BS (MBS or SBS), UE, and Resource Block (RB) are indexed with b, m, and n, respectively. In addition, we assume that UL and DL bandwidths, BW_{UL} and BW_{DL}, are divided into a number of equal size RBs (with bandwidth of BW_{RB}). Table 2 shows the notations used in our paper.

2-4- Channel Model and SINR

Let $|h_{bm}^n|^2$ denote the channel gain between b'th BS (BS_b) and m'th UE (UE_m) in n'th RB (RB_n). This channel gain includes path loss and shadowing (large scale and small scale fading). The path loss model depends on the distance between BS_b and UE_m (D_{bm}) and path loss exponent γ. If we denote S_{bm}^n to present the shadowing effect, then $S_{bm}^n \times D_{bm}^{-\gamma} = |h_{bm}^n|^2$. In this study we set $\gamma = 3$.

We assume that noise and signal of UEs are mutually statistically independent. In addition, the signals of interfering UEs and the signal of desired UE are also independent. Thus, SINR of UE_m in DL and UL transmission in RB_n are obtained as [25, 27]

$$\mathrm{SINR}_{bmn}^{DL} = \frac{p_{bmn}^{DL}|h_{bm}^n|^2}{\sum_{\substack{b'\in\mathcal{B},m'\in\mathcal{U}\\ b'\neq b,m'\neq m}} p_{b'm'n}^{DL}|h_{b'm}^n|^2+\sigma^2} \tag{5}$$

Table 2. Notations used in this paper.

Notation	Description	Notation	Description
$\lvert h_{bm}^{n}\rvert^2$	Channel power gain between UE m and BS b in RB n	D_{bm}	Distance between BS b and UE m
x_{bm}^{n}	DL binary association variable	y_{bm}^{n}	UL binary association variable
p_{bmn}^{DL}	Transmit power of BS b to UE m in RB n	p_{bmn}^{UL}	Transmit power of UE m to BS b in RB n
$\mathcal{B}$	Set of BSs	σ^2	Noise power
$R_m^{QoS_{DL}}$	DL QoS minimum rate for UE m	$R_m^{QoS_{UL}}$	UL QoS minimum rate for UE m
$P_{DL_b}^{max}$	Maximum transmit power of BS b	$P_{UL_m}^{max}$	Maximum transmit power of UE m
C_b^{DL}	Capacity of BS b in DL mode	C_b^{UL}	Capacity of BS b in UL mode
λ	Regulation parameter	A	A positive large number
$\mathrm{BW}_{mmWave}^{DL}$	mmWave DL bandwidth	$\mathrm{BW}_{mmWave}^{UL}$	mmWave UL bandwidth
$C_{ONU_i}^{DL,UL}$	Capacity of ONU i in DL (UL)	$\mathcal{U}$	Set of UEs
Λ	Number of wavelengths	O	Number of ONUs served by OLT
c_{PON}^{DL}	PON data rate in DL	c_{PON}^{UL}	PON data rate in UL
S_{bm}^{n}	Shadowing effect between UE_m and BS_b in RB_n	$\mathcal{R}$	Set of resource blocks

$$\mathrm{SINR}_{bmn}^{UL} = \frac{p_{bmn}^{UL}\lvert h_{bm}^{n}\rvert^2}{\sum_{\substack{b'\in\mathcal{B},m'\in\mathcal{U}\\ b'\neq b,m'\neq m}} p_{b'm'n}^{UL}\lvert h_{bm'}^{n}\rvert^2+\sigma^2} \quad (6)$$

where p_{bmn}^{DL} (or p_{bmn}^{UL}) is the transmit power of BS_b (or UE_m) in RB n. The achievable rate of each UE in nats/s/Hz in RB n at UL and DL, R_{bmn}^{UL} and R_{bmn}^{DL}, are given by

$$R_{bmn}^{UL} = \log\left(1+\mathrm{SINR}_{bmn}^{UL}\right), \quad (7)$$

$$R_{bmn}^{DL} = \log\left(1+\mathrm{SINR}_{bmn}^{DL}\right). \quad (8)$$

3- Problem Formulation

In this section, we formulate the optimization problem of decoupled UL and DL user association, RB allocation, and power control of BSs and UEs, which is henceforth referred to as Decoupled Resource Allocation Problem (DRAP). The objective of the problem is sum-rate maximization, and we consider the backhaul capacity limitation and minimum required transmission rate of UEs as QoS requirements. The DRAP is formulated as follows

$$\textbf{P1}: \max_{x,y,p^{DL},p^{UL}} \sum_{b\in\mathcal{B},m\in\mathcal{U},n\in\mathcal{R}} \left(x_{bm}^{n}R_{bmn}^{DL} + y_{bm}^{n}R_{bmn}^{UL}\right) \quad (9)$$

$$\text{s.t.} \quad \sum_{b\in\mathcal{B},n\in\mathcal{R}} \left(x_{bm}^{n}R_{bmn}^{DL}\right) \geq R_m^{QoS_{DL}}, \quad m\in\mathcal{U}, \quad (10)$$

$$\sum_{b\in\mathcal{B},n\in\mathcal{R}} \left(y_{bm}^{n}R_{bmn}^{UL}\right) \geq R_m^{QoS_{UL}}, \quad m\in\mathcal{U}, \quad (11)$$

$$\sum_{b\in\mathcal{B},n\in\mathcal{R}} x_{bm}^{n} = 1, \quad m\in\mathcal{U}, \quad (12)$$

$$\sum_{b\in\mathcal{B},n\in\mathcal{R}} y_{bm}^{n} = 1, \quad m\in\mathcal{U}, \quad (13)$$

$$\sum_{m\in\mathcal{U}} x_{bm}^{n} \leq 1, \quad b\in\mathcal{B}, n\in\mathcal{R}, \quad (14)$$

$$\sum_{m\in\mathcal{U}} y_{bm}^{n} \leq 1, \quad b\in\mathcal{B}, n\in\mathcal{R}, \quad (15)$$

$$\sum_{m\in\mathcal{U},n\in\mathcal{R}} \left(x_{bm}^{n}R_{bmn}^{DL}\right) \leq C_b^{DL}, \quad b\in\mathcal{B}, \quad (16)$$

$$\sum_{m\in\mathcal{U},n\in\mathcal{R}} \left(y_{bm}^{n}R_{bmn}^{UL}\right) \leq C_b^{UL}, \quad b\in\mathcal{B}, \quad (17)$$

$$p_{bmn}^{DL} \le P_{DL_b}^{max} x_{bm}^{n}, \quad b \in \mathcal{B}, m \in \mathcal{U}, n \in \mathcal{R}, \tag{18}$$

$$p_{bmn}^{UL} \le P_{UL_m}^{max} y_{bm}^{n}, \quad b \in \mathcal{B}, m \in \mathcal{U}, n \in \mathcal{R}, \tag{19}$$

$$x_{bm}^{n}, y_{bm}^{n} \in \{0,1\}, \quad b \in \mathcal{B}, m \in \mathcal{U}, n \in \mathcal{R}, \tag{20}$$

where (9) is the objective of DRAP maximizing the sum-rate of FiWi-HetNet. We note that vectors $\boldsymbol{x}, \boldsymbol{y}, \boldsymbol{p}^{DL}$, and $\boldsymbol{p}^{UL}$ contain x_{bm}^{n}, y_{bm}^{n}, p_{bmn}^{DL}, and p_{bmn}^{UL} (for $b \in \mathcal{B}, m \in \mathcal{U}, n \in \mathcal{R}$), respectively. Constraints (10) and (11) assure the DL and UL minimum rate of UE_m (referred to as QoS constraint), (12) and (13) limit the association of each UE to only one BS, (14) and (15) guarantee allocation of a RB to only one UE. Constraints (16) and (17) indicate that the sum rate of UEs connected to BS_b in UL and DL transmission must be less than the UL and DL capacity of the backhaul link of BS_b, i.e., C_b^{UL} and C_b^{UL}, respectively. Constraints (18) and (19) ensure that when $x_{bm}^{n}=1$ and $y_{bm}^{n}=1$, the p_{bmn}^{DL} and p_{bmn}^{UL} can be at most P_{DL}^{max} and P_{UL}^{max}, respectively, otherwise, if $x_{bm}^{n}=0$ ($y_{bm}^{n}=0$) BS_b (UE_m) does not transmit any signal in RB_n.

It is worth mentioning that problem **P1** is a class of Mixed-Integer Nonlinear Programming (MINLP) that jointly investigates user association, RB allocation, and power control problem in both UL and DL. As **P1** is MINLP, and hence, non-convex, obtaining its solution is quite challenging and intractable. Thus, in the next section, we will propose an algorithm to solve it sup-optimally. It should be noted that as the variables and constraints of DL and UL do not relate to each other, we can separate **P1** into two sub-problems, one for UL (**P1.1**) and another for DL (**P1.2**) user association and resource allocation. The sub-problems **P1.1** and **P1.2** are given by

$$\begin{aligned}&\mathbf{P1.1}: \max_{\boldsymbol{x},\boldsymbol{p}^{DL}} \textstyle\sum_{b\in\mathcal{B},m\in\mathcal{U},n\in\mathcal{R}} x_{bm}^{n} R_{bmn}^{DL}\\ &\mathbf{s.t.}: (10),\ (12),\ (14),\ (16),\ (18),\ \mathbf{x} \in \{0,1\}.\end{aligned} \tag{21}$$

$$\begin{aligned}&\mathbf{P1.2}: \max_{\boldsymbol{y},\boldsymbol{p}^{UL}} \textstyle\sum_{b\in\mathcal{B},m\in\mathcal{U},n\in\mathcal{R}} y_{bm}^{n} R_{bmn}^{UL}\\ &\mathbf{s.t.}: (11),\ (13),\ (15),\ (17),\ (19),\ \mathbf{y} \in \{0,1\}.\end{aligned} \tag{22}$$

It is worth mentioning that by considering the following constraint in (23), the decoupled UL and DL association in **P1** is changed to the coupled association, which is the conventional approach used in the existing RAN technologies.

$$\textstyle\sum_{n\in\mathcal{R}} y_{bm}^{n} = \sum_{n\in\mathcal{R}} x_{bm}^{n} \quad m \in \mathcal{U}, b \in \mathcal{B}. \tag{23}$$

It should be noted that the constraint (23) holds only when a user is connected to the same BS in both DL and UL, because when user m connects to BS b in DL (on any RB), the right hand side of (23) becomes "1" implying that the left hand side should be "1" too. We define problem **P2** to optimize the coupled UL and DL association, RB allocation, and power control, as a benchmark to evaluate the decoupling gain in FiWi-HetNet. The problem **P2** is obtained by including the constraint (23) in **P1**, thus we have

$$\begin{aligned}&\mathbf{P2}: \max_{\boldsymbol{x},\boldsymbol{y},\boldsymbol{p}^{UL},\boldsymbol{p}^{DL}} \textstyle\sum_{b\in\mathcal{B},m\in\mathcal{U},n\in\mathcal{R}}\\ &(x_{bm}^{n} R_{bmn}^{DL} + y_{bm}^{n} R_{bmn}^{UL})\end{aligned} \tag{24}$$

4- The Proposed Algorithm

In this section, we propose a 2-step iterative approach inspired from [27, 34, 35] to solve the problems **P1** and **P2**. In the first step, we solve the user association (UA) sub-problem by considering fixed values for data transmission powers to find the association variables. In the second step, the power allocation subproblem is solved by using the results of the previous step (association variables) as fixed values to obtain data transmission powers. Then, in the next iteration, the obtained data transmission powers are used in the first sub-problem. This procedure is continued until the results meet a convergence condition, as explained in the next sub-sections.

4-1- User Association Sub-problem

First, we relax binary optimization variables x_{bm}^{n} and y_{bm}^{n} to be real value within $[0,1]$ and add a regulation term to recover binary values. Therefore, in order to investigate the association of users, we solve the following problem

$$\begin{aligned}&\mathbf{P3.1}: \max_{\boldsymbol{x},\boldsymbol{y}} \textstyle\sum_{b\in\mathcal{B},m\in\mathcal{U},n\in\mathcal{R}} x_{bm}^{n} R_{bmn}^{DL} + y_{bm}^{n} R_{bmn}^{UL} -\\ &\lambda(x_{bm}^{n} - x_{bm}^{n\,2} + y_{bm}^{n} - y_{bm}^{n\,2})\end{aligned} \tag{25}$$

$$\begin{aligned}&\mathbf{s.t.} \quad R_{bmn}^{DL} + \left(1 - x_{bm}^{n}\right) A \ge R_m^{QoS_{DL}},\\ &b \in \mathcal{B}, m \in \mathcal{U}, n \in \mathcal{R},\end{aligned} \tag{26}$$

$$\begin{aligned}&R_{bmn}^{UL} + \left(1 - y_{bm}^{n}\right) A \ge R_m^{QoS_{UL}},\\ &b \in \mathcal{B}, m \in \mathcal{U}, n \in \mathcal{R},\end{aligned} \tag{27}$$

$$\mathbf{x}, \mathbf{y} \in [0,1] \tag{28}$$

$$(12), (13), (14), (15), (16), (17), (23).$$

It should be noted that **P3.1** is obtained by considering constant values for transmit power of devices in **P2** or **P1**, where for **P1** we must remove constraint (13) in **P3.1**. Thus, the problem **P3.1** finds only the association variables for fixed values of transmit powers. In addition, since we have relaxed the binary association variables in (28), we added a regulation term in the objective function of **P3.1**. In fact, the regulation term is considered to force the optimization to converge to integer solution in which for $\lambda >> 1$ the results of the relaxed problem will be the same as the main problem [25].

In other words, the parameter λ controls the importance of the regulation term in the objective function. For $\lambda >> 1$ the regulation term will force the relaxed variables to converge to one or zero. In addition, we use (26) and (27) instead of (10) and (11) in **P1**, because in this step, the data transmission powers are fixed and we should start from a feasible point at the initialization of the algorithm. However, by using (26) and (27) this issue is resolved. We note that A is a large positive constant, i.e. $A >> 1$, thus in case of $x_{bm}^{n} = 0$, the constraint will be $A > R_{m}^{QoS}$ that is true always, and when $x_{bm}^{n} = 1$ the term consisting A will disappear so that the constraint will be $R_{bmn} \geq R_{m}^{QoS}$, thus (26) and (27) assure the same limitation as (10) and (11), respectively.

Clearly the problem **P3.1** is a non-convex nonlinear programming, which can be transformed into a linear convex problem using successive convex approximation (SCA) [23, 24, 36] on the regulation term, which forces relaxed binary variables to be 0 or 1. To apply the SCA method, a lower bound is computed for the regulation term. Note that for a convex function $f(x)$ we have $f(x) \geq f(x_0) + f'(x_0)(x - x_0)$, where $f'(x_0)$ is the first derivative of $f(x)$ evaluated at point x_0. The lower bound of $f(x)$ is affine and can be used to approximate $f(x)$ in the maximization problem using the SCA method. In **P3.1**, the regulation term is convex, thus its lower bound is given by

$$\lambda\left({x_{bm}^{n}}^{2} - x_{bm}^{n} + {y_{bm}^{n}}^{2} - y_{bm}^{n}\right) \geq \lambda\begin{pmatrix} {x_{val_{bm}}^{n}}^{2} - x_{val_{bm}}^{n} + {y_{val_{bm}}^{n}}^{2} - y_{val_{bm}}^{n} + \\ \left(2x_{val_{bm}}^{n} - 1\right)\left(x_{bm}^{n} - x_{val_{bm}}^{n}\right) + \\ \left(2y_{val_{bm}}^{n} - 1\right)\left(y_{bm}^{n} - y_{val_{bm}}^{n}\right) \end{pmatrix}. \quad (29)$$

where $x_{val_{bm}}^{n}$ and $y_{val_{bm}}^{n}$ are the solutions obtained in the previous iteration of the 2-step algorithm by solving the following linear convex problem **P3.2**. Note that **P3.2** is obtained by using the lower bound of the regulation term which is affine.

$$+\left(2x_{val_{bm}}^{n} - 1\right)\left(x_{bm}^{n} - x_{val_{bm}}^{n}\right) + \left(2y_{val_{bm}}^{n} - 1\right)\left(y_{bm}^{n} - y_{val_{bm}}^{n}\right))) \quad (30)$$

$$\textbf{s.t.} \quad (12)-(17),\ (23),\ (26),\ (27),\ (28).$$

The problem **P3.2** is convex and can be easily solved by optimization solvers such as cvx [36, 37]. After obtaining the association variables, in the next iteration, the transmit powers of BSs and UEs are allocated as described in the following.

4-2- Power Allocation Sub-problem

After solving the user association sub-problem in **P3.1**, the values of **x** and **y** are inserted into **P1** (or **P2**), and by removing the association constraints in **P1**, the power allocation sub-problem is defined as follows

$$\textbf{P3.3}: \max_{\boldsymbol{p}^{UL},\boldsymbol{p}^{DL}} \sum_{b\in\mathcal{B},m\in\mathcal{U},n\in\mathcal{R}} \left(x_{bm}^{n} R_{bmn}^{DL} + y_{bm}^{n} R_{bmn}^{UL}\right)$$

$$\textbf{s.t.}: (10),\ (11),\ (16),\ (17),\ (18),\ (19).$$

The problem **P3.3** is non-convex. To solve **P3.3**, we use the following lemma for posynomial functions. It is worthy to note that a posynomial function for real value variables x_1, x_2, ..., x_n is in the form of $F(x_1, x_2, \ldots, x_n) = \sum_{k=1}^{K} f_k(x_1\ x_2\ \ldots\ x_n)$, where $f_k(x_1, x_2, \ldots, x_n) = c_k x_1^{a_{1k}} \cdots x_n^{a_{nk}}$ is a monomial function, K is the upper bound of the summation, $c_k \geq 0$, and $a_{ik} \in \mathbb{R}$.

Lemma 1 *Let* $g(x) = \sum_i u_i(x)$ *be a posynomial function, then* ($g(x) \geq \tilde{g}(x) = \prod_i \left(\frac{u_i(x)}{\alpha_i}\right)^{\alpha_i}$ ($\sum_i \alpha_i = 1$) *) is the Arithmetic-Geometric Mean Approximation (AGMA) of g(x). If* $\alpha_i = \frac{u_i(x_0)}{g(x_0)}$ *then it will be the best local minimum approximation [26].*

Proof. Consider Arithmetic Mean Geometric Mean (AM-GM) inequality, $\sum_i \alpha_i v_i \geq \prod_i v_i^{\alpha_i}$. If we take $u_i = \alpha_i v_i$, then $\sum_i u_i \geq \prod_i \left(\frac{u_i}{\alpha_i}\right)^{\alpha_i}$ and the equality holds when $\alpha_i = \frac{u_i}{\sum_i u_i}$. Thus, by using AGMA, the sub-problem **P3.3** is changed as follows

$$\textbf{P3.4}: \min_{\boldsymbol{p}^{DL},\boldsymbol{p}^{UL}} \prod_{b\in\mathcal{B},m\in\mathcal{U},n\in\mathcal{R}} \left(\frac{\sigma^2 + \sum_{b'\in\mathcal{B},m'\in\mathcal{U}b'\neq b,m'\neq m} p_{b'm'n}^{DL} |h_{b'm}^{n}|^2}{D}\right)^{x_{bm}^{n}} \times \prod_{b\in\mathcal{B},m\in\mathcal{U},n\in\mathcal{R}} \left(\frac{\sigma^2 + \sum_{b'\in\mathcal{B},m'\in\mathcal{U}b'\neq b,m'\neq m} p_{b'm'n}^{UL} |h_{bm'}^{n}|^2}{\tilde{D}}\right)^{y_{bm}^{n}}$$

$$\textbf{s.t.} \prod_{b\in\mathcal{B},n\in\mathcal{R}} \left(\frac{\sigma^2 + \sum_{\substack{b'\in\mathcal{B},m'\in\mathcal{U} \\ b'\neq b,m'\neq m}} p_{b'm'n}^{DL} |h_{b'm}^{n}|^2}{D}\right)^{x_{bm}^{n}} \leq e^{-R_m^{QoS_{DL}}},\ m \in \mathcal{U}, \quad (31)$$

$$\prod_{b\in\mathcal{B},n\in\mathcal{R}} \left(\frac{\sigma^2 + \sum_{\substack{b'\in\mathcal{B},m'\in\mathcal{U} \\ b'\neq b,m'\neq m}} p_{b'm'n}^{UL} |h_{bm'}^{n}|^2}{\tilde{D}}\right)^{y_{bm}^{n}} \leq e^{-R_m^{QoS_{UL}}},\ m \in \mathcal{U}, \quad (32)$$

$$\prod_{m\in\mathcal{U},n\in\mathcal{R}} \left(\frac{\sigma^2+\sum_{\substack{b'\in\mathcal{B},m'\in\mathcal{U}\\ b'\neq b,m'\neq m}} p^{DL}_{b'm'n}|h^{n}_{b'm}|^2}{D'}\right)^{x^n_{bm}} \le e^{C^{DL}_b}, b\in\mathcal{B}, \tag{33}$$

$$\prod_{m\in\mathcal{U},n\in\mathcal{R}} \left(\frac{\sigma^2+\sum_{\substack{b'\in\mathcal{B},m'\in\mathcal{U}\\ b'\neq b,m'\neq m}} p^{UL}_{b'm'n}|h^{n}_{bm'}|^2}{\widetilde{D}'}\right)^{y^n_{bm}} \le e^{C^{UL}_b}, b\in\mathcal{B}, \tag{34}$$

$$(18),\ (19).$$

where D, D', $\tilde{D}$, $\widetilde{D'}$ are given by

$$\widetilde{D} = \theta_{bn}^{\theta_{bn}^{-1}} \prod_{b'\in\mathcal{B},m'\in\mathcal{U}} \left(\frac{p^{UL}_{b'm'n}|h^n_{bm'}|^2}{p^{UL-val}_{b'm'n}|h^n_{bm'}|^2/\theta_{bn}}\right)^{\frac{p^{UL-val}_{b'm'n}|h^n_{bm'}|^2}{\theta_{bn}}},$$

$$D = \theta_{mn}^{\theta_{mn}^{-1}} \prod_{b'\in\mathcal{B},m'\in\mathcal{U}} \left(\frac{p^{DL}_{b'm'n}|h^n_{b'm}|^2}{p^{DL-val}_{b'm'n}|h^n_{b'm}|^2/\theta_{mn}}\right)^{\frac{p^{DL-val}_{b'm'n}|h^n_{b'm}|^2}{\theta_{mn}}},$$

$$D' = \theta_{bmn}'^{\theta_{bmn}'^{-1}} \prod_{\substack{b'\in\mathcal{B},m'\in\mathcal{U}\\ b'\neq b,m'\neq m}} \left(\frac{p^{DL}_{b'm'n}|h^n_{b'm}|^2}{p^{DL-val}_{b'm'n}|h^n_{b'm}|^2/\theta_{bmn}'}\right)^{\frac{p^{DL-val}_{b'm'n}|h^n_{b'm}|^2}{\theta_{bmn}'}},$$

$$\widetilde{D}' = \theta_{bmn}''^{\theta_{bmn}''^{-1}} \prod_{\substack{b'\in\mathcal{B},m'\in\mathcal{U}\\ b'\neq b,m'\neq m}} \left(\frac{p^{UL}_{b'm'n}|h^n_{bm'}|^2}{p^{UL-val}_{b'm'n}|h^n_{bm'}|^2/\theta_{bmn}''}\right)^{\frac{p^{UL-val}_{b'm'n}|h^n_{bm'}|^2}{\theta_{bmn}''}}.$$

where θ_{mn}, θ_{bn}, θ_{bmn}', θ_{bmn}'' are defined as

$$\theta_{mn} = \sigma^2 + \sum_{b'\in\mathcal{B},m'\in\mathcal{U}} p^{DL-val}_{b'm'n}|h^n_{b'm}|^2, \tag{35}$$

$$\theta_{bn} = \sigma^2 + \sum_{b'\in\mathcal{B},m'\in\mathcal{U}} p^{UL-val}_{b'm'n}|h^n_{bm'}|^2, \tag{36}$$

$$\theta_{bmn}' = \sigma^2 + \sum_{\substack{b'\in\mathcal{B},m'\in\mathcal{U}\\ b'\neq b,m'\neq m}} p^{DL-val}_{b'm'n}|h^n_{b'm}|^2, \tag{37}$$

$$\theta_{bmn}'' = \sigma^2 + \sum_{\substack{b'\in\mathcal{B},m'\in\mathcal{U}\\ b'\neq b,m'\neq m}} p^{UL-val}_{b'm'n}|h^n_{bm'}|^2. \tag{38}$$

where $p^{UL-val}_{b'm'n}$ and $p^{DL-val}_{b'm'n}$ are respectively the values of transmit powers of the UEs and BSs obtained in the previous iteration (i.e., the power control sub-problem). It can be proved that the problem **P3.4** is a geometric programming (GP) [36]. As expressed in [38], a GP has a general form as follows

$$\begin{aligned} &\min_{x} \quad f_0(x) \\ &\textbf{s.t.} \quad f_i(x)\le 1, \quad i=1,\dots,m, \\ &\quad g_i(x)=1, \quad i=1,\dots,p, \end{aligned} \tag{39}$$

where f_i, g_i are posynomial and monomial functions, respectively, and x is the optimization variable. In order to prove that **P3.4** is a GP, we show that the objective function of **P3.4** is posynomial. In addition, since the right hand side of all constraints in **P3.4** are constant, we can rewrite all constraints in the form of $f_i(x)\le 1$. The objective function and left hand side of all constraints (19a)-(19d) are the multiplication of liner terms (e.g., in the form of $f(x_1,x_2)=(\sigma^2+x_1)(\sigma^2+x_2)=x_1x_2+\sigma^2(x_1+x_2)+\sigma^4$). Thus, the objective function and constraints (19a)-(19d) are the summation of monomial functions (i.e., posynomial). Furthermore, the constraints (18) and (19) are monomial functions (a spacial case of posynomial) in terms of $\boldsymbol{p}^{DL}, \boldsymbol{p}^{UL}$. Consequently, **P3.4** is a GP. The whole process to solve **P1** or **P2** sub-optimally is summarized in Algorithm 1. In this algorithm, first, the values of transmit powers in DL and UL are initialized to maximum value. Then, the problem **P3.2** is solved at line 2 to find the association vectors **x** and **y**. At line 3, we apply the following heuristic relation

$$x^n_{val_{bm}} = x^*_{b,m,n} = \begin{cases} 1 & if \ \ (b,n)=\operatorname*{argmax}_{(b',n')} x^{n'}_{b'm} \\ 0 & otherwise. \end{cases} \tag{40}$$

The main reason to use (40) is to speed up the simulations by removing small value variables. For example, when the solution of the first sub-problem is [0.99 0.001 0.009], we can reduce the run time of the algorithm by setting small value variables to be zero and consider [1 0 0] for the next step. It should be noted that in line 3, $\boldsymbol{y}^*$ is obtained by applying (40) on the values of $y_{b,m,n}$. The power allocation sub-problem **P3.4** is solved in line 4 to find the sub-optimal values of transmit powers. This procedure is iteratively continues until the objective function meets the convergence condition. The convergence condition is that the difference of the objective function in two consequent iterations to be less than $\epsilon = 0.001$. It is worth mentioning that in our simulations we did not observe any performance loss by using equation (40).

5- Numerical Results

In this section, we evaluate the proposed algorithms numerically. We assume that the MBS and SBSs' locations are fixed and UEs are uniformly distributed in 2-D plane, as shown in Fig. 2.

The optimization variables and simulation parameters are listed in Table 3.

Fig. 3(a) shows the sum rate of network in nats/s/Hz versus the backhual capacity of BSs for decoupled uplink/downlink association (DUDA) and coupled uplink/downlink association (CUDA) modes. We observe that the sum rate in the CUDA scenario is lower than that of DUDA one. In

Algorithm 1. User Association, and Power and RB Allocation.

Algorithm 1 User Association, and Power and RB Allocation

Input: Channel response (h), network topology

Output: $p^{*DL}, p^{*UL}, x^{*}, y^{*}$

Initialization: $p^{DL-val} = p_{DL}^{max}, p^{UL-val} = p_{UL}^{max}$

while Convergence **do**

  Solve **P3.2** until its convergence to obtain **x, y** for fixed p^{DL-val}, p^{UL-val}

  Obtain x^{*} and y^{*} from (40)

  Solve **P3.4** to obtain optimal p^{DL}, p^{UL} for fixed association variables

end while

return: $p^{*DL}, p^{*UL}, x^{*}, y^{*}$

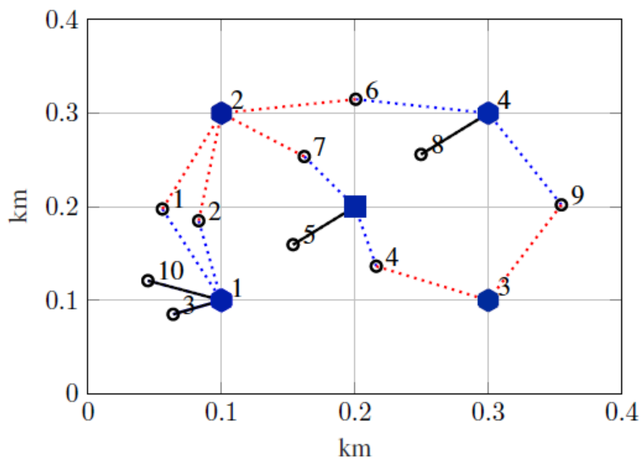

Fig. 2. Network topology with 10 UEs distributed uniformly in x and y-axes shown as black circles, 4 SBSs indicated as blue hexagonal, and one MBS depicted as blue squares. The red dotted lines show UL links, blue dotted lines are DL links, and the black lines indicate both DL and UL links (i.e., coupled association).

addition, as the backhaul capacity becomes larger the network throughput increases.

Fig. 3(b) illustrates the sum-rate of network in terms of the number of RBs allocated in either DL or UL. We observe that in both CUDA and DUDA, the sum rate of network increases as the number of RBs goes higher. In addition, results reveal that by applying the UL/DL decoupled association the sum rate is improved, where the decoupling gain is higher for a lower number of RBs. This is due to the fact that at larges number of RBs, the inference power coming from neighbor users or BSs is canceled since the orthogonal channels are increased than before.

In Fig. 3(c) the effect of the minimum required transmission rate (QoS constraint) has been evaluated. As shown in Fig. 5(c), we observe that the sum-rate decreases as the minimum required transmission rate (R_{min}) of UEs becomes larger. This is due to the fact that with the increase of R_{min} the feasible region of the optimization problem is restricted and its optimum value is changed. We can also conclude that the decoupling gain is higher as R_{min} decrease.

It is worth mentioning that we can consider different values for R_{min} of each UE, and realize a multi-class of the service access network. The practical application of this approach is to support machine-type communication in the internet of things (IoT) application besides ordinary cellular communications. IoT sensors have limited battery and need low rate transmission, whereas ordinary UEs need a higher transmission rate and can consume more power. Thus, by selecting appropriate R_{min} for IoT sensors and ordinary UEs, we can support both IoT sensors and UEs in the proposed FiWi-HetNets.

To evaluate the effect of different backhaul technologies in the throughput of FiWi-HetNet, we considered three PON conFigurations with splitting ratios of 64, 128, and 256, where each ONU is connected to an MBS and each MBS support 4 SBSs. In addition, we assume that the number of UEs in these scenarios is 10×64, 10×128, and 10×256 UEs. In addition, for simplicity, only the DL transmission is considered and the QoS constraint is ignored. In Fig. 4, the average throughput per MBS and its corresponding SBSs (aerial throughput supported by each ONU) are shown for various GPON standards. We observe that for the splitting ratio of 256, the throughput is increased linearly as we upgrade PON technology from GPON to NG-PON2, however, for splitting ratios of 128 and 64, the XG-PON and NG-PON2 have the same throughput which is higher than that of GPON. This saturation is due to the fact that in a low splitting ratio, the

Table 3. Parameters used in simulations

Parameter	Value
Number of MBSs	1
Number of SBSs	4
Number of UEs	10
Path loss coefficient	$\gamma = 3$
Wireless DL BH Capacity	$C_{-}^{DL} = 8$ nats/s/Hz
Wireless UL BH Capacity	$C_{-}^{UL} = 8$ nats/s/Hz
Minimum QoS DL Rate	$R_{-}^{QoS_{DL}} = 0.2$ nats/s/Hz
Minimum QoS UL Rate	$R_{-}^{QoS_{UL}} = 0.2$ nats/s/Hz
Noise Power	$\sigma^2 = 1$ (normalized)
Maximum UL Power	$P_{UL}^{max} = 1e6$ (60 dB) normalized to noise power
Maximum DL Power	$P_{DL}^{max} = 1e7$ (70 dB) for SBSs, $P_{DL}^{max} = 5e7$ (76.98 dB) for MBS
Number of DL (UL) RBs	$N = 4$
Regulation parameter	$\lambda = 10$
Resource block bandwidth	200 kHz
BH bandwidth	Number of RBs × RB bandwidth

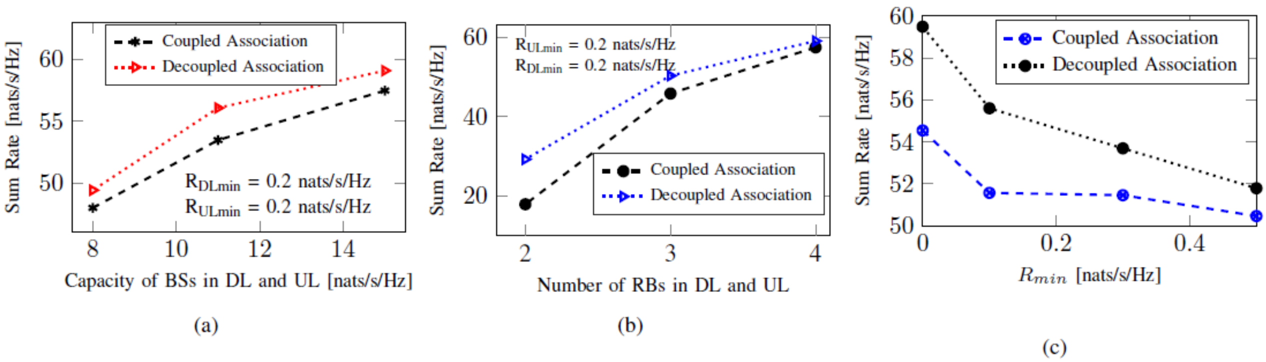

Fig. 3. (a) Sum Rate vs the backhaul capacity of BSs for the DUDA and CUDA modes, (b) Sum Rate vs the number of RBs in DL (UL) for the DUDA and CUDA modes, (c) Sum Rate vs minimum required DL and UL transmission rates ($R_{min} = R_{UL}^{QoS} = R_{DL}^{QoS}$), for the DUDA and CUDA modes.

backhaul capacity of MBS is higher than its capacity at the air-interface and as a result upgrading PON technology from XG-PON to NG-PON2 does not affect its performance.

3- Conclusion

In this paper, we investigated the optimization problem of decoupled DL/UL user association, RB allocation, and power control in FiWi-HetNet by considering the backhaul capacity limitation and minimum required transmission rate. As the formulated optimization problem is MINLP, we separated it into two sub-problems and solved them iteratively. We also evaluated the effect of backhhaul capacity on the sum rate

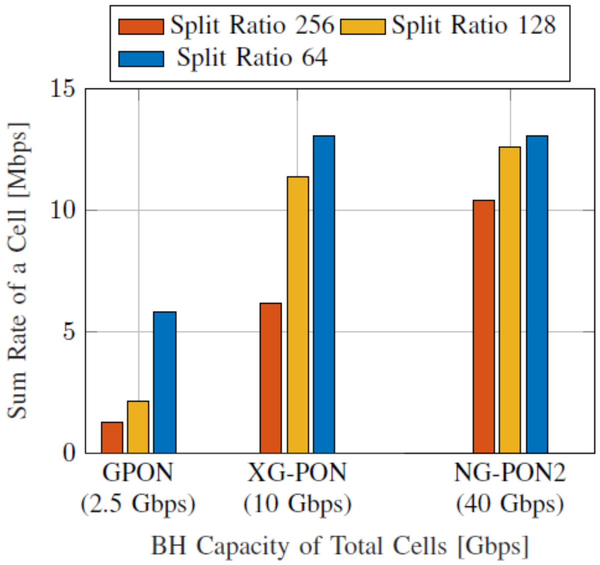

Fig. 4. Sum Rate of the MBS and its corresponding SBSs vs the capacity of fiber backhaul provided by various GPON standards.

of FiWi-HetNet and showed that as long as the traffic load of MBS is higher than its backhaul capacity, upgrading its backhaul improves the network throughput. For the cases in which the traffic load of MBS is lower than its backhaul capacity, the network throughput is saturated to the backhaul capacity, and upgrading backhaul technology does not improve the FiWi-HetNet throughput.

3- References

[1] M. Maier, M. Chowdhury, B.P. Rimal, D.P. Van, The tactile internet: vision, recent progress, and open challenges, *IEEE Communications Magazine*, 54(5) (2016) 138-145.

[2] J.G. Andrews, S. Buzzi, W. Choi, S.V. Hanly, A. Lozano, A.C.K. Soong, J.C. Zhang, What will 5G be?, *IEEE Journal on selected areas in communications*, 32(6) (2014) 1065-1082.

[3] M. ITU-R, Minimum requirements related to technical performance for IMT-2020 radio interface (s), in, Nov, 2017.

[4] FSAN Roadmap, in, \url{https://www.fsan.org/roadmap/ }.

[5] D. Nesset, PON roadmap [invited], *IEEE/OSA Journal of Optical Communications and Networking*, 9(1) (2017) A71-A76.

[6] N. Ghazisaidi, M. Maier, Fiber-wireless (FiWi) access networks: Challenges and opportunities, *IEEE Network*, 25(1) (2011) 36-42.

[7] H. Beyranvand, W. Lim, M. Maier, C. Verikoukis, J.A. Salehi, Backhaul-aware user association in FiWi enhanced LTE-A heterogeneous networks, *IEEE Transactions on Wireless Communications*, 14(6) (2015) 2992-3003.

[8] J. Liu, H. Guo, H. Nishiyama, H. Ujikawa, K. Suzuki, N. Kato, New Perspectives on Future Smart FiWi Networks: Scalability, Reliability, and Energy Efficiency, *IEEE Communications Surveys Tutorials*, 18(2) (2016) 1045-1072.

[9] A.G. Sarigiannidis, M. Iloridou, P. Nicopolitidis, G. Papadimitriou, F.N. Pavlidou, P.G. Sarigiannidis, M.D. Louta, V. Vitsas, Architectures and Bandwidth Allocation Schemes for Hybrid Wireless-Optical Networks, *IEEE Communications Surveys Tutorials*, 17(1) (2015) 427-468.

[10] B.P. Rimal, M. Maier, Mobile data offloading in FiWi enhanced LTE-A heterogeneous networks, *Journal of Optical Communications and Networking*, 9(7) (2017) 601-615.

[11] D.P. Van, B.P. Rimal, M. Maier, L. Valcarenghi, Design, analysis, and hardware emulation of a novel energy conservation scheme for sensor enhanced FiWi networks (ECO-SFiWi), *IEEE Journal on Selected Areas in Communications*, 34(5) (2016) 1645-1662.

[12] J.G. Andrews, Seven ways that HetNets are a cellular paradigm shift, *IEEE Communications Magazine*, 51(3) (2013) 136-144.

[13] M. Jaber, M.A. Imran, R. Tafazolli, A. Tukmanov, 5G Backhaul Challenges and Emerging Research Directions: A Survey, *IEEE Access*, 4 (2016) 1743-1766.

[14] U. Siddique, H. Tabassum, E. Hossain, D.I. Kim, Wireless backhauling of 5G small cells: challenges and solution approaches, *IEEE Wireless Communications*, 22(5) (2015) 22-31.

[15] G. Zhang, T.Q.S. Quek, M. Kountouris, A. Huang, H. Shan, Fundamentals of heterogeneous backhaul design—Analysis and optimization, *IEEE Transactions on Communications*, 64(2) (2016) 876-889.

[16] J.E. Mitchell, Integrated Wireless Backhaul Over Optical Access Networks, *Journal of Lightwave Technology*, 32(20) (2014) 3373-3382.

[17] F. Boccardi, J. Andrews, H. Elshaer, M. Dohler, S. Parkvall, P. Popovski, S. Singh, Why to decouple the uplink and downlink in cellular networks and how to do it, *IEEE Communications Magazine*, 54(3) (2016) 110-117.

[18] S. Singh, X. Zhang, J.G. Andrews, Joint rate and SINR coverage analysis for decoupled uplink-downlink biased cell associations in HetNets, *IEEE Transactions on Wireless Communications*, 14(10) (2015) 5360-5373.

[19] H.-S. Jo, Y.J. Sang, P. Xia, J.G. Andrews, Heterogeneous cellular networks with flexible cell association: A comprehensive downlink SINR analysis, *IEEE Transactions on Wireless Communications*, 11(10) (2012) 3484-3495.

[20] H. Elshaer, M.N. Kulkarni, F. Boccardi, J.G. Andrews, M. Dohler, Downlink and uplink cell association with traditional macrocells and millimeter wave small cells, *IEEE Transactions on Wireless Communications*, 15(9) (2016) 6244-6258.

[21] L. Zhang, W. Nie, G. Feng, F.-C. Zheng, S. Qin, Uplink Performance Improvement by Decoupling Uplink/Downlink Access in HetNets, *IEEE Transactions on Vehicular Technology*, 66(8) (2017) 6862-6876.

[22] S. Sekander, H. Tabassum, E. Hossain, Decoupled uplink-downlink user association in multi-tier full-duplex cellular networks: A two-sided matching game, *IEEE Transactions on Mobile Computing*, 16(10) (2017) 2778-2791.

[23] Q. Ye, B. Rong, Y. Chen, M. Al-Shalash, C. Caramanis, J.G. Andrews, User association for load balancing in heterogeneous cellular networks, *IEEE Transactions on Wireless Communications*, 12(6) (2013) 2706-2716.

[24] H.H.M. Tam, H.D. Tuan, D.T. Ngo, T.Q. Duong, H.V. Poor, Joint load balancing and interference management for small-cell heterogeneous networks with limited backhaul capacity, *IEEE Transactions on Wireless Communications*, 16(2) (2017) 872-884.

[25] B. Khamidehi, A. Rahmati, M. Sabbaghian, Joint sub-channel assignment and power allocation in heterogeneous networks: An efficient optimization method, *IEEE Communications Letters*, 20(12) (2016) 2490-2493.

[26] M. Chiang, C.W. Tan, D.P. Palomar, D. O'neill, D. Julian, Power control by geometric programming, *IEEE Transactions on Wireless Communications*, 6(7) (2007) 2640-2651.

[27] D.T. Ngo, S. Khakurel, T. Le-Ngoc, Joint subchannel assignment and power allocation for OFDMA femtocell networks, *IEEE Transactions on Wireless Communications*, 13(1) (2013) 342-355.

[28] D. Nesset, NG-PON2 Technology and Standards, *Journal of Lightwave Technology*, 33(5) (2015) 1136-1143.

[29] ITU, G .984: Gigabit-capable Passive Optical Networks (GPON): General characteristics, *ITU-T, March*, (2008).

[30] I. SG15, 10-Gigabit-capable passive optical networks (XG-PON), ITU-T Standard G-Series G. 987. x (. 1-. 4), Jan 2010, in.

[31] ITU, G. 989:40-Gigabit-capable passive optical networks (NG-PON2): General requirements, in, 2013.

[32] F. Aurzada, M. L\'evesque, M. Maier, M. Reisslein, FiWi Access Networks Based on Next-Generation PON and Gigabit-Class WLAN Technologies: A Capacity and Delay Analysis, *IEEE/ACM Transactions on Networking*, 22(4) (2014) 1176-1189.

[33] S. Singh, M.N. Kulkarni, A. Ghosh, J.G. Andrews, Tractable Model for Rate in Self-Backhauled Millimeter Wave Cellular Networks, *IEEE Journal on Selected Areas in Communications*, 33(10) (2015) 2191-2211.

[34] S. Parsaeefard, R. Dawadi, M. Derakhshani, T. Le-Ngoc, Joint user-association and resource-allocation in virtualized wireless networks, *IEEE Access*, 4 (2016) 2738-2750.

[35] S. Parsaeefard, R. Dawadi, M. Derakhshani, T. Le-Ngoc, M. Baghani, Dynamic Resource Allocation for Virtualized Wireless Networks in Massive-MIMO-Aided and Fronthaul-Limited C-RAN, *IEEE Transactions on Vehicular Technology*, 66(10) (2017) 9512-9520.

[36] S. Boyd, L. Vandenberghe, Convex optimization, Cambridge university press, 2004.

[37] M. Grant, S. Boyd, Y. Ye, CVX: Matlab software for disciplined convex programming, in, 2008.

[38] S. Boyd, S.-J. Kim, L. Vandenberghe, A. Hassibi, A tutorial on geometric programming, *Optimization and engineering*, 8(1) (2007) 67.

HOW TO CITE THIS ARTICLE

R. Hashemi, H. Beyranvand, Backhaul-aware Decoupled Uplink and Downlink User Association, and Power Control in Fi-Wi HetNets, AUT J. Elec. Eng., 52(2) (2020) 147-158.

DOI: 10.22060/eej.2020.18115.5343